http://dx.doi.org/10.5012/bkcs.2013.34.11.3456

Notes

Control of the Shell Thickness of TiO_2@SiO_2 Particles and Its Surface Functionalization

Junho Ahn, Sung Ho Jung, Ji Ha Lee, Ki-Young Kwon,* and Jong Hwa Jung*

Department of Chemistry and Research Institute of Natural Sciences, Gyeongsang National University, Jinju 660-701, Korea
**E-mail: jonghwa@gnu.ac.kr (J. H. Jung); KYKwon@gnu.ac.kr (K.-Y. Kwon)*
Received June 5, 2013, Accepted August 2, 2013

Key Words : Functionalization, Yolk-shell type, Particles, TiO_2@SiO_2

The fabrication of functional hollow particles is of great scientific and technological interest for purposes of applications ranging from drug delivery, coatings, photonic devices, and nanoscale reaction vessels.[1-3] Various methods, including approaches such as spray drying, emulsion templating techniques, and self-assembly processes, have been described for the preparation of hollow spheres out of latex, metal, and inorganic materials.[4-11]

Among the various structures of these particles, the core-shell structure is a powerful platform for controlled release, confined nanocatalysis and optical and electronic applications.[12] A hybrid of the core-shell structure, termed the yolk-shell or rattle-type structure, is a special class of core-shell structures with a distinctive core@void@shell configuration which has attracted great interest in recent years.[13-15] With the unique properties of movable cores, interstitial hollow spaces, and the functionalization of the shells, yolk-shell structures have great potential for application in various fields, including nanoreactors, biomedicine, lithium-ion batteries, and photocatalysis.[16-20] Although various yolk-shell structures with different types of cores and different particle sizes have been successfully prepared, the control of shell thickness of yolk-shell type particles has been less well studies.[21-23] Therefore, the investigation of the control of thickness and crystalline structure of yolk-shell type particles is valuable. Here we report the control of shell thickness in yolk-shell particles. The crystalline structure of the yolk-shell particle has also been characterized by annealing at different temperatures.

The route for the preparation of yolk-shell (TiO_2@SiO_2) titanium-silica particles is given in Scheme 1. After being dried in an oven at 50 °C for 2 h, titanium particles can be coated with silica under Stöber conditions. Silica coating of the dried titanium results in TiO_2@SiO_2 particles. Upon calcination at 600-625 °C for 15-60 min, the greater porosity of the titanium cores of TiO_2@SiO_2 particles causes them to shrink more than the silica component and gives rise to TiO_2@SiO_2 particles.

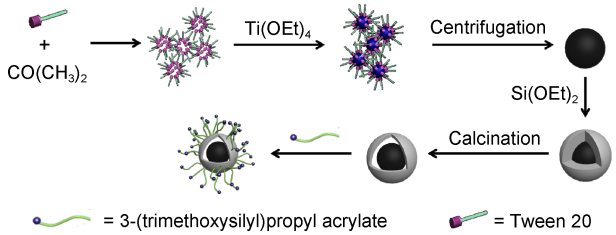

Scheme 1. Synthetic route of a yolk@shell type acryl functionalized TiO_2@SiO_2 particles.

A TEM micrograph of the bare titanium particles is given in Figure 1(a) and the TiO_2@SiO_2 particles, which display the shrinkage that occurred after calcination, are shown in Figure 1(b). We found the size of the particles to be 650-680 nm (5% polydispersity) and the shell thickness to be 100-120 nm, with an inner core of 340-360 nm. The void between the shrunken core and the silica shell was 70-130 nm depending on the particle size and the calcination time.

To corroborate that the synthesized particles have SiO_2 layers, an elemental analysis was conducted to identify the presence of Si and SiO_2 in the particles.[24] The EDX analysis showed that the TiO_2@SiO_2 core/shell particles consisted of Ti:Si in the ratio of 41:11% (Figure S1). Furthermore, FTIR studies were also conducted to determine the presence of specific functional groups and intra and/or intermolecular interactions between various groups in the sample (Figure S2). The FTIR spectrum of pure TiO_2 particles after calcination at 600 °C showed distinctive vibrational bands about 500-600 cm^{-1}, known to be the asymmetric, symmetric and bending modes of Ti–O–Ti, respectively (Figure S2(a)).[25] However, a new band at 958 cm^{-1}, attributed to the vibrational stretching band of Ti–O–Si, was observed in addition to the three bands of Si–O–Si in the FTIR spectrum of TiO_2@SiO_2 particles after calcination at 600 °C (Figure S2(b)). This further supports the conclusion that Si was

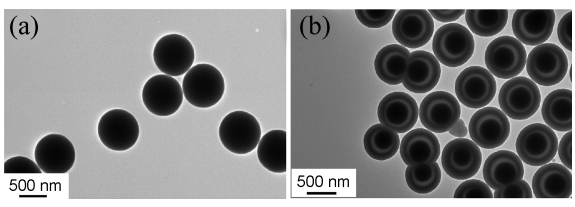

Figure 1. TEM images of (a) dried TiO_2 particles at 50 °C and (b) TiO_2@SiO_2 particles after calcination at 600 °C for 15 min.

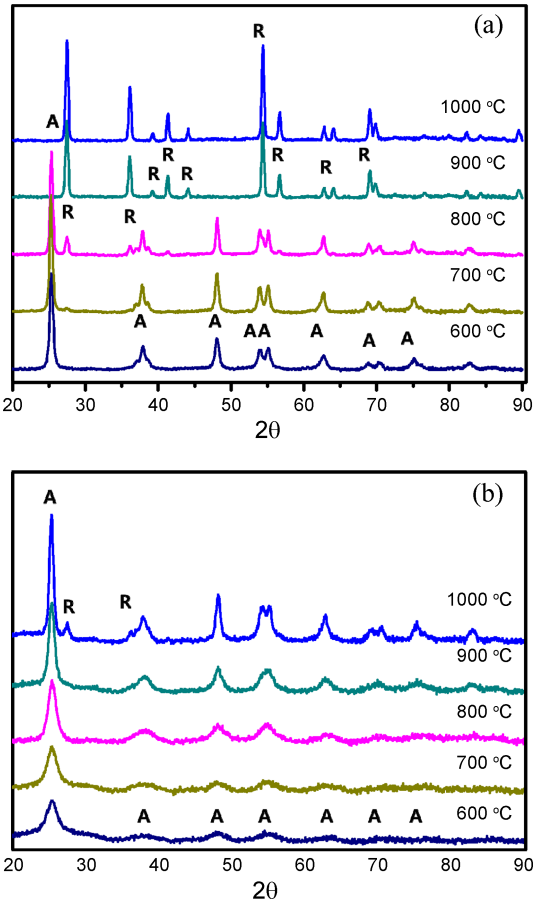

Figure 2. The XRD patterns of (a) TiO_2 particles and (b) TiO_2@SiO_2 particles; A: anatase, and R: rutile.

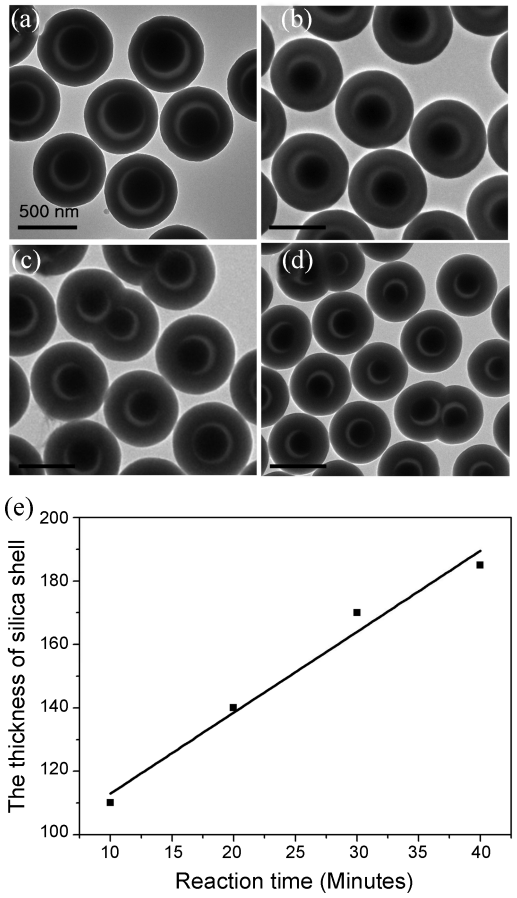

Figure 3. TEM images of TiO_2@SiO_2 particles by changing the reaction time in reactor; (a) 10, (b) 20, (c) 30 and (d) 40 minutes. (e) The plot for the average thickness of silica shell against reaction time. Scale bar: 500 nm.

covalently bonded to the surface of TiO_2 nanospheres, thus forming TiO_2@SiO_2 nanospheres.[26]

To further analyze the crystalline behavior of the TiO_2@SiO_2 particles with respect to the ratios of Ti:Si obtained at different calcination temperatures, we employed X-ray diffraction (XRD) and the results are shown in Figure 2(a) and 2(b), respectively. The XRD patterns of the particles show that all the peaks became narrower by heating which indicated a greater degree of crystallinity of these TiO_2@SiO_2 particles. Furthermore, the XRD pattern of the hollow particles annealed at 800 °C showed new peaks for the rutile phase of TiO_2 at around this temperature, in addition to the peaks from the anatase phase. The synthesized particles in this study also showed very similar behavior to the phase change of bulk TiO_2, from anatase to rutile structures. The phase change temperature of the TiO_2@SiO_2 particles was slightly higher than that of bulk TiO_2 particles. The phase transition was also observed by FT IR spectroscopy (Figure S3). The vibration peak of the Ti-O bond appeared at 588 cm^{-1} at the calcination temperature of 800 °C. On the other hands, after treatment at 900 °C, the vibrational peak of the Ti-O bond appeared at 625 cm^{-1} (Figure S3(a) and Figure S3(b)), because the bond length of Ti-O of the anatase form is longer than that of the rutile form.[27] In comparison of the wavenumber of Ti-O peak from the TiO_2 and TiO_2@SiO_2 particles against the calcination temperature, TiO_2@SiO_2 particles showed relatively higher anatase phase stabilities than the pure TiO_2 particles (Figure S3(b) and Figure S3(d)).

The thickness of the shell layer of TiO_2@SiO_2 particles was controlled by the reaction times. As shown in Figure 3, the thickness of shell layer of the particles increased. For dried titanium, the deposition of the silica occurred mainly on the surface of the TiO_2 nanoparticles. The shortest shell thickness is *ca.* 50-60 nm when the TiO_2 is not fully dried. However, shell thickness is *ca.* 100-120 nm when TiO_2 was thoroughly dried. TiO_2@SiO_2 prepared from dried TiO_2 was more shrank than that of TiO_2@SiO_2 prepared from undried one. In spite of large shrinkage, the surface area of TiO_2@SiO_2 prepared from dried TiO_2 after calcination showed of 250 m^2/g (Figure S4).[28]

Finally, since inorganic-organic hybrid materials offer much versatility, we attached a functional group onto the surface of TiO_2@SiO_2 particles. Methoxysilyl propyl acrylate (MPA) as the organic matrix was used to provide the inorganic-organic hybrid materials, acrylated TiO_2@SiO_2 particles. We observed the FTIR spectra of the TiO_2@SiO_2 particles before and after attachment of MPA by covalent bond. A noticeable distinction between the FTIR spectrum of the acrylated TiO_2@SiO_2 particles and that of pure TiO_2@SiO_2

particles was the absence of the band around 1735 cm^{-1}, corresponding to the carbonyl group, -C=O of MPA, bound to the TiO_2@SiO_2 particles (Figure S5). This data also further supports the presence of MPA covalently bound on the surface of the TiO_2@SiO_2 particles. In addition, we performed elemental mapping by energy dispersive X-ray spectroscopy (EDX) technique coupled with TEM measurements. After attachment of MPA, the material (Figure S6(a)) contained silicon (Figure S6(b)), titanium (Figure S6(c)), carbon (Figure S6(d)), and oxygen (Figure S6(e)) components. These findings strongly support the view that the MPA was immobilized onto the surface of the SiO_2 layer.

In our preliminary study, we have photo-polymerized the acrylated TiO_2@SiO_2 particles onto the surface of polyacrylic acid using UV irradiation. The particles were homogeneously attached onto polyacrylic acid, as observed by the TEM images. These results support the idea that the TiO_2@SiO_2 hybrid particles could act as a new additive to enhance several physical properties, such as mechanical strength and reflectivity.

In conclusion, TiO_2@SiO_2 yolk/core shell particles were obtained by a sol-gel polymerization. The shell thickness of TiO_2@SiO_2 can successfully be controlled by sol-gel reaction times. The anatase structure of TiO_2@SiO_2 was more stable than that of TiO_2 particles calcinated at higher temperature. Moreover, acrylate-functionalized TiO_2@SiO_2 particles were also successfully synthesized using the TiO_2@SiO_2 particles as building blocks by copolymerization of trimethoxysilyl groups of MPA with the existing hydroxyl groups on the surface of TiO_2@SiO_2 particles. Furthermore, TEM, EDX, and FTIR studies confirmed that MPA had been successfully grafted to the surface of TiO_2@SiO_2 particles. Finally, we believe that the present results showing the development of surface functionalized particles can be very useful in the fields of various functional applications, and could be extended to more sophisticated hybrid materials.

Experimental

Preparation of TiO_2 Particles.[29] Two solutions were prepared: 0.45 wt % of titanium butoxide in ethylene glycol and 2.03 mM of surfactant (Tween 20) in acetone containing a small amount of water. The titanium butoxide solution was mixed with the Tween 20 solution. After stirring for 1 day at room temperature, solution was centrifuged for 10 min at 3000 rpm.

Preparation of TiO_2@SiO_2 Particles.[29] TiO_2 particles (0.082 g) were dried for 2 h at 323 K. The particles were dispersed in 100 mL of ethanol under the sonication and then 5 mL of aqueous ammonia solution was added to the dispersion. Tetraethyl orthosilicate (TEOS) (2 mL) was added to the dispersion. After stirring for 10-40 min at room temperature, the solvent was removed by centrifugation at 3000 rpm for 5 min. The resulting powder was calcinated at 873-1273 K for 15 minutes.

Preparation of Acryl Functionalized TiO_2@SiO_2 Particles. TiO_2@SiO_2 particles were dispersed in a solution of 1.5 mL of ethanol, 1.7 mL of water and 1.25 mL of aqueous ammonia solution under sonication for 10 min. 3-(Trimethoxysilyl)-propyl acrylate (0.1 mL) was added to the solution. The solution was stirred for 1 day and the particles were collected by centrifugation at 3000 rpm for 10 min. The resulting particles were washed with ethanol and dried in vacuum.

Acknowledgments. This work was supported by NRF (2012-002547), and Environmental-Fusion Project (191-091-004), Korea. In addition, this work was partially supported by a grant from the Next-Generation BioGreen 21 Program (SSAC, grant#: PJ009041022012), Rural development Administration, Korea.

Supporting Information. FT-IR spectra, TEM images, and BET data of TiO_2@SiO_2 particles.

References

1. Pekarek, K. J.; Jacob, J. S.; Mathiowitz, E. *Nature* **1994**, *367*, 258.
2. Lou, X. W.; Archer, L. A.; Yang, Z. *Adv. Mater* **2008**, *20*, 3987.
3. Huang, C.; Huang, W.; Yeh, C. *Biomaterials* **2011**, *32*, 556.
4. Lu, Y.; Fan, H.; Stump, A.; Ward, T. L.; Rieker, T.; Brinker, C. J. *Nature* **1999**, *398*, 223.
5. Schacht, S.; Huo, Q.; Voigt-Martin, I. G.; Stucky, G. D.; Schuth, F. *Science* **1996**, *273*, 768.
6. Discher, B. M.; Won, Y. Y. D. S.; Ege, J.; Lee, C. M.; Bates, F. S.; Discher, D. E.; Hammer, D. A. *Science* **1999**, *284*, 1143.
7. Caruso, F.; Caruso, R. A.; Möhwald, H. *Science* **1998**, *282*, 1111.
8. Zhong, Z.; Yin, Y.; Gates, B.; Xia, Y. *Adv. Mater.* **2000**, *12*, 206.
9. Wu, D.; Ge, X.; Zhang, Z.; Wang, M.; Zhang, S. *Langmuir* **2004**, *20*, 5192.
10. Joo, J. B.; Zhang, Q.; Lee, I.; Dahl, M.; Zaera, F.; Yin, Y. *Adv. Funct. Mater.* **2012**, *22*, 166.
11. Zhang, T.; Ge, J.; Hu, Y.; Zhang, Q.; Aloni, S.; Yin, Y. *Angew. Chem. Int. Ed.* **2008**, *47*, 5806.
12. Chaudhuri, R. G.; Paria, S. *Chem. Rev.* **2012**, *112*, 2373.
13. Wu, X.; Xu, D. *Adv. Mater.* **2010**, *22*, 1516.
14. Wu, X.; Xu, D. *J. Am. Chem. Soc.* **2009**, *131*, 2774.
15. Wong, Y. J.; Zhu, L.; Teo, W. S.; Tan, Y. W.; Yang, Y.; Wang, C.; Chen, H. *J. Am. Chem. Soc.* **2011**, *133*, 11422.
16. Li, L.; Tang, F.; Liu, H.; Liu, T.; Hao, N.; Chen, D.; Teng, X.; He, J. *ACS. Nano*. **2010**, *4*, 6874.
17. Lee, J.; Park, J. C.; Song, H. *Adv. Mater.* **2008**, *20*, 1523.
18. Liu, J.; Qiao, S. Z.; Hartono, S. B.; Lu, G. Q. *Angew. Che. Int. Ed.* **2010**, *49*, 4981.
19. Liu, J.; Qiao, S. Z.; Chen, J. S.; Lou, X. W.; Xing, X.; Lu, G. Q. *Chem. Commun.* **2011**, *47*, 12578.
20. Ikeda, S.; Ikoma, Y.; Kobayashi, H.; Harada, T.; Torimoto, T.; Ohtani, B.; Matsumura, M. *Chem. Commun*. **2007**, *36*, 3753.
21. Liu, J.; Xu, J.; Che, R.; Chen, H.; Liu, M.; Liu, Z. *Chem. Eur. J.* **2013**, *19*, 6746.
22. Fang, Q.; Xuan, S.; Jiang, W.; Gong, X. *Adv. Funct. Mater.* **2011**, *21*, 1902.
23. Wang, Y.; Wang, F.; Chen, B.; Xu, H.; Shi, D. *Chem. Commun.* **2011**, *47*, 10350.
24. Williams, D. D. B.; Carter, C. B. *Transmission Electron Microscopy*; Springer: 1996.
25. Murashkevich, A. N.; Lavitskaya, A. S.; Barannikova, T. L.; Zharskii, I. M. *J. Appl. Spectrosc*. **2008**, *75*, 730.
26. Lee, C. G.; Ahn, A.; Lee, S. J.; Lee, J.; Choi, M. Y.; Jung, J. H. *J. Nanosci. Nanotecnol*. **2011**, *11*, 3696.
27. Linsebigler, A. L.; Lu, G.; Yates, J. T. *Chem. Rev.* **1995**, *95*, 735.
28. Demirörs, A. F.; Blaaderen, A. V.; Imhof, A. *Chem. Mater.* **2009**, *21*, 979.
29. Stöber, W.; Fink, A.; Bohn, E. *J. Colloid Interface Sci.* **1968**, *26*, 62.